Massive Integration of Wind Power at Distribution Level Supported by Battery Energy Storage Systems

Juan. M. Lujano-Rojas,
José A. Domínguez-Navarro,
and José M. Yusta
Univ. Zaragogoza, Zaragoza, Spain
lujano.juan@gmail.com; jadona@unizar.es;
jmyusta@unizar.es

Gerardo J. Osório
C-MAST/UBI,
Covilha,
Portugal
gjosilva@gmail.com

Mohamed Lotfi and João P. S. Catalão
Faculty of Engineering of the University of
Porto (FEUP) and INESC TEC, Porto
4200-465, Portugal
mohd.f.lotfi@gmail.com;
catalao@fe.up.pt

***Abstract*—Integration of renewable generation in distribution systems aims to reduce consumption of energy from conventional sources such as coal and oil in order to minimize the negative impacts of the human ecological footprint. Massive incorporation of renewables can produce reverse power flow at distribution substations, which is against the operating philosophy and design of energy systems. To deal with this problem, the installation of a battery energy storage system (BESS) is proposed in this work. Incorporation of BESS at distribution substations can manage the excess of renewable power generation flowing in reverse, adding flexibility to the power system and allowing increased distributed generation capacity to be installed. Optimal sizing of vanadium redox flow batteries (VRFBs) is carried out by using golden section search algorithm considering capital costs as well as operating and maintenance costs over the project lifetime. The effectiveness of the proposed technique is evaluated through the analysis of a case study. A significant reduction of both reverse flow and the power to be supplied by the substation has been observed.**

***Index Terms*—Battery energy storage system, Distributed generation, Golden section search algorithm, Smart grid.**

I. NOMENCLATURE

a, b, c	Parameters of wind turbine model.
ACC	Annualized capital cost (€/yr).
AMC	Annualized maintenance cost (€/yr).
ARC	Annualized replacement cost (€/yr).
CF	Cost factor (%).
CRF	Capital recovery factor.
d, g	Parameters of charge controller model.
E_B	Rated capacity of VRFB (kWh).
E_B^{max}	Maximum VRFB capacity considered (kWh).
E_B^{min}	Minimum VRFB capacity considered (kWh).
η_B	Efficiency of VRFB.
$\eta_{I(t)}$	Efficiency of power converter at time t.
F	Control factor of charge controller.
h, k	Parameters of power converter.
$K_{S(t)}$	Electricity price time series (€/MWh).
K_S^{max}	Peak electricity price (€/MWh).
$L_{(n,t)}$	Load demand at node n at time t (kVA).
n	Index for each node of DS ($n = 1, \dots, N$).
P_B^{max}	Cell stack rating power (kW).
$P_{B(t)}$	Battery power at time t (kW).
$P_{DS(t)}$	Power of DS at time t (kW).
$P_{I(t)}$	Power of converter at time t (kW).
P_I^{max}	Rated power of converter (kW).
$P_{SU(t)}$	Power of substation at time t (kW).
P_W^{max}	Rated power of wind turbine (kW).
$P_{W(t)}$	Power of wind turbine at time t (m/s).
$R_{(t)}$	Reference time series at time t.
SOC_B^{max}	Maximum SOC setting.
SOC_B^{min}	Minimum SOC setting.
$SOC_{(t)}$	SOC at time t.
$TRX_{(n)}$	Power of transformer at node n (kVA).
t	Index for time ($t = 1, \dots, T$; T = 8760 h).
v_O	Cut-off wind speed of wind turbine (m/s).
v_I	Cut-in wind speed of wind turbine (m/s).
v_R	Rated wind speed of wind turbine (m/s).
$v_{(t)}$	Wind speed at time t (m/s).

II. INTRODUCTION

Adoption of renewable generation at the residential level is an alternative means of supplying energy using local, clean, and natural resources. The majority of common renewable resources (e.g. wind and solar) are intermittent and thus present challenges to be adapted to the traditional operating philosophy and design of distribution systems.

Nevertheless, the transformation of current distribution systems (DS) to smart grids (SG) is solving many technical problems associated with the integration of distributed generation (DG) and battery energy storage systems (BESSs), in addition to enabling the implementation of dynamic pricing strategies and other demand response programs [1].

Incorporation of BESS to enhance the interaction between SG and DG has been widely discussed in the literature, in order to achieve sustainable adoption of renewable resources from a techno-economical perspective.

Recently in [2], several aspects related to residential consumers' behavior have been considered for the operation of load aggregators, presumed electricity market players. A multi-layer operating strategy based on multi-agent simulation has been used to determine the magnitude of incentives to be offered to consumers.

In [3], management of BESSs has been studied for the operation of DS by solving the optimal power flow (OPF) problem through a dual-horizon rolling scheduling technique. Factors such as energy import and export, renewable generation (and the associated forecasting error), as well as load demand behavior have been taken into account.

Similarly, in [4], the influence of load demand (and renewable generation) forecasting error has been considered in the optimal control of BESSs to maximize economic benefit. The proposed strategy is a two-level framework to reduce the prediction error effect during real-time operating conditions.

In [5], BESS charging and discharging processes were widely investigated for peak load shaving, power curve smoothing, and voltage regulation. In [6], BESS optimal sizing and placement were used to develop an algorithm based on OPF with convex relaxation of load flow expressions.

Massive DG penetration in DS can manifest reverse power flow associated with excess renewable generation. Reverse power flow creates DS operational problems for installed protection systems and voltage regulators, as well as problems for Bulk system power generation ramping and scheduling [7].

In this context, this work proposes the installation of BESS based on a vanadium redox flow battery (VRFB) to mitigate the magnitude of reverse power flow. The proposed method is formulated as an optimization problem to minimize the net present cost (NPC) of VRFB adoption operating in a DS with high share of wind generation.

Golden section search algorithm (GSSA) has been chosen to determine the optimal capacity of VRFB, taking into account the influence of charge controller and power converter on VRFB performance.

This manuscript is organized as follows: In Section III the energy system mathematical model is described. In Section IV the BESS optimal sizing strategy is explained. In Section V the proposed methodology is illustrated by means of a case study. Finally, conclusions are discussed in Section VI.

III. Model of the Power System

Fig. 1 illustrates the generalized structure of the power system under analysis, which should incorporate a substation, a BESS, and a dump load. The dump load consumes excess energy available when renewable resources are abundant, load demand is low, and BESS is fully charged.

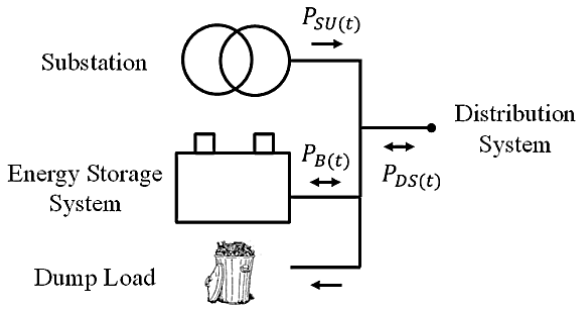

Figure 1. Scheme of the energy system under study.

BESS consists of a VRFB operating in parallel with the substation to store excess renewable energy generated to be later supplied to DS, reducing substation power generation. In this way, excess energy is cycled through the BESS and used to supply DS load demand.

A. Distributed Wind Generation

DG considered in this work is based on a wind generator with reactive power compensation, as shown in Fig. 2. It is assumed that wind turbines (WTs) operate at unity power factor $\left(Q_{W(t)} \leftarrow 0 \; \forall \; t = 1, \dots, T\right)$. This takes advantage of all active power produced, while the reactive power compensator produces or consumes reactive power to maintain connection point voltage at a value equal to the DS rated voltage.

The WT has been represented using the general-purpose model developed in [8], which is described in Eqs. (1)-(4). Provision of reactive power is assumed to be based on a distribution static compensator [9].

$$P_{W(t)} = \begin{cases} 0, 0 \le v_{(t)} \le v_I, v_I > v_O \\ a + b\left(v_{(t)}\right) + c(v_{(t)})^2, v_I \le v_{(t)} \le v_R \\ P_W^{max}, v_R \le v_{(t)} \le v_O \end{cases} \quad (1)$$

$$a = \frac{1}{(v_I - v_R)^2}\left[v_I(v_I + v_R) - 4v_I v_R \left(\frac{v_I + v_R}{2v_R}\right)^3\right] \quad (2)$$

$$b = \frac{1}{(v_I - v_R)^2}\left[4(v_I + v_R)\left(\frac{v_I + v_R}{2v_R}\right)^3 - (3v_I + v_R)\right] \quad (3)$$

$$c = \frac{1}{(v_I - v_R)^2}\left[2 - 4\left(\frac{v_I + v_R}{2v_R}\right)^3\right] \quad (4)$$

The amount of reactive power $\left(Q_{C(t)} \; \forall \; t = 1, \dots, T\right)$ has been calculated from the power flow solution, considering the connection point as a voltage-controlled node. In this context, the solution gives us the reactive power to be injected or consumed from DS to maintain voltage at its nominal value.

More specific details can be found in [10]. The efficiency of the interconnection transformer has been assumed to be close to unity, since its effect on the performance of DG has not been taken into account in this study.

B. Vanadium Redox Flow Battery

The structure of BESS is shown in Fig. 3, where the storage technology (VRFB), charge controller, and power converter have been incorporated.

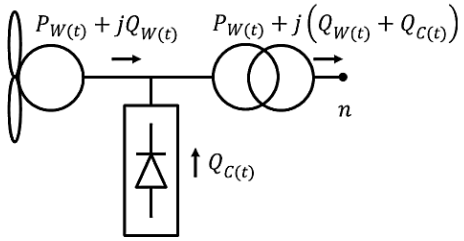

Figure 2. Architecture of the wind turbine connected to DS.

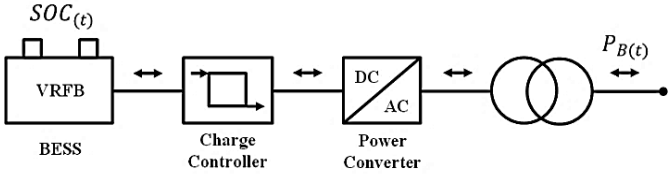

Figure 3. Scheme of the BESS.

VRFB is mathematically represented using Eq. (5) [11] as an approximation of the battery state of charge (SOC). Several factors have been considered: charging $(P_{B(t)} > 0)$ or discharging $(P_{B(t)} < 0)$, power, conversion efficiency (η_B),, and the influence of the charge controller (F).

$$SOC_{(t)} = SOC_{(t-1)} + \frac{P_{B(t)}}{E_B}\eta_B F \tag{5}$$

The effects of the charge controller on the operation of VRFB are modeled in Eq. (5) by means of the control factor (F), which is defined in Eq. (6) [11].

$$F = \begin{cases} max\left(1 - e^{\left[\left(\frac{d}{P_{B(t)}/P_B^{max}+g}\right)\left(SOC_{(t)} - SOC_B^{max}\right)\right]}\right), P_{B(t)} > 0 \\ 1, P_{B(t)} < 0 \end{cases} \tag{6}$$

This expression models actions taken by the charge controller to maintain the SOC less than or equal to its maximum recommended value by the VRFB manufacturer (SOC_B^{max}), and preventing VRFB over-discharge by disconnecting it from the DS in order to maintain the SOC greater than or equal to its minimum setting (SOC_B^{min}).

The power converter was modeled based on its variable efficiency as represented in Eq. (7) [11]. Typically, the efficiency decreases as power decreases, which directly impacts the interaction between BESS and the rest of DS.

$$\eta_{I(t)} = \frac{P_{I(t)}}{hP_I^{max} + (1+k)P_{I(t)}} \tag{7}$$

C. Smart Grid

This study considers a SG operating with a real-time pricing scheme [12]. Load demand and electricity prices are assumed to be proportional. These assumptions allow the formulation of a simplified representation of the load demand and electricity price time series for each node of DS. These time series could be estimated by applying the procedure described as follows:

- Step 1: Obtain a time series of electricity prices (or load demand) for the time period of interest $(t = 1, \dots, T)$. These series can reveal important information about the behavior of consumers and throughout the day.
- Step 2: The series found in Step 1 is scaled in order to obtain a time series of T elements in the interval [0,1]. This is the reference time series $\left(R_{(t)} \forall\, t = 1, \dots, T\right)$.
- Step 3: Once the reference time series has been estimated, load demand time series at a determined node (n) is calculated by using Eq. (8),

$$L_{(n,t)} = TRX_{(n)}R_{(t)}\ \forall\, t = 1, \dots, T \tag{8}$$

This assumes that load demand reaches its maximum or minimum values simultaneously for all nodes, which could correspond to an extreme operating condition.

- Step 4: The electricity prices time series is obtained by scaling the reference time series according to a determined yearly peak price, as shown in Eq. (9),

$$K_{S(t)} = K_S^{max}R_{(t)}\ \forall\, t = 1, \dots, T \tag{9}$$

IV. BESS Sizing

As previously mentioned, BESS is designed to mitigate reverse power flow at substation. To achieve this goal, the proposed procedure is described as follows:

- Step 1: Perform a probabilistic power flow analysis [10] without considering the influence of BESS. The active power to be supplied by the substation will have positive and negative value. Positive power values are provided by the substation and represented by the variable $(P_{SU(t)}\ \forall\, t = 1, \dots, T)$, while the negative power values (reverse power flow) are dissipated by the dump load. The VFRB cell stack rated capacity (P_B^{max}) is estimated as the maximum power dissipated by the dump load.
- Step 2: Set the converter rated power equal to the VFRB cell stack rated power $(P_B^{max} = P_I^{max})$.
- Step 3: Consider the limit values of VRFB capacity $(E_B^{min}$ and $E_B^{max})$ as the GSSA optimization constraints.
- Step 4: Apply GSSA [13], [14] over this interval in order to minimize NPC, as defined in Eq. (10), being the objective function of the optimization problem [15],

$$NPC = \left(ACC + ARC + AMC + \sum_{t=1}^{T} K_{S(t)}P_{SU(t)}\right)\Big/CRF \tag{10}$$

The objective function takes into account the VFRB capital cost (ACC), replacement cost (ARC), maintenance cost (AMC), and costs related to energy obtained by the utility under real-time pricing conditions.

V. Case Study

The proposed methodology is illustrated by analyzing the small DS shown in Fig. 4, which was modified from the original one in [16]. Information about the system topology, impedances, and transformer capacities $(TRX_{(n)}\ \forall\, n = 1, \dots, N = 15)$ is shown in Table I. The WT (installed at node 15) rated capacity is 1 MW $(P_W^{max} = 1\ \text{MW})$.

Hourly performance of the system is analyzed for a one-year period. Probabilistic power flow analysis parameters are listed in Table II. Wind speed resource data of Eindhoven meteorological station of the year 2005 has been used [17]. Wind speed time series and corresponding probability distribution are shown in Fig. 5 and 6, respectively. The mean wind speed is 4.0408 m/s.

Using electricity prices of the Spanish market of the year 2016 [18], the reference time series $\left(R_{(t)}\ \forall\, t = 1, \ldots, 8760\right)$ plotted in Fig. 7 has been obtained.

This series has been combined with the transformer power shown in Table I $\left(TRX_{(n)}\ \forall\, n = 1, \ldots, 14\right)$, and the peak electricity price assumed in Table II ($K_S^{max} = 120$ €/MWh), in order to account for dynamic characteristics of load demand and energy prices in a typical year.

VRFB component costs reported in [19] were considered, where total costs were estimated at approximately 310 €/kWh. The charge controller and power converter of BESS were modeled by assuming: $d = 20.73, g = 0.55,\ h = 0.0119$, and $k = 0.0155$, respectively [11].

With the case study constructed, a sensitivity analysis has been carried out using GSSA by introducing the cost factor (CF) as a percentage of VRFB capital cost. CF values close to 0% (CF←0) represent VRFBs with negligible capital cost, while values closer to 100% (CF←1) reflect actual capital costs of the storage system.

In Fig. 7 it is observed how normalized load and price (reference time series), remains low during the beginning of the year until the middle ($0\ h \le t \le 4000\ h$, approx.) and increases at a constant rate onwards ($t \le 4000\ h$).

The sensitivity analysis results are shown in Fig. 8. They show that VRFB is only viable when its acquisition cost is very low ($CF \leftarrow 0$). As capital cost increases, the adoption of VRFB loses economic sustainability very rapidly ($CF \leftarrow 1$).

To investigate performance of VRFB adoption from a technical perspective, optimization results are shown for the most favorable case to install the storage system ($CF \leftarrow 0$).

Fig. 9 shows the convergence of GSSA from both extremes of the interval $\left[E_B^{min},\ E_B^{max}\right]$. Maximum capacity considered was 50 MWh ($E_B^{max} = 50$ MWh), while the minimum was adjusted to 0 kWh $\left(E_B^{min} = 0\ \text{kWh}\right)$.

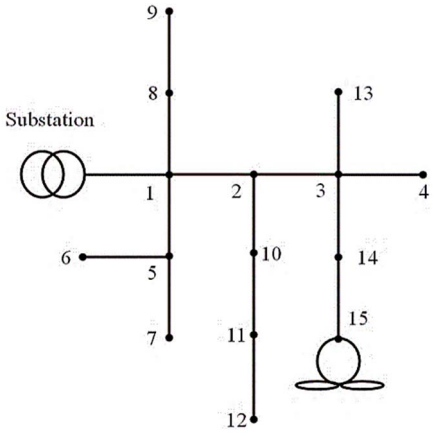

Figure 4. Distribution system under analysis

TABLE I. DISTRIBUTION SYSTEM INFORMATION

Sending Node	Receiving Node	Resistance (Ω)	Reactance (Ω)	Transformer Power (kVA)
Substation	1	1.35309	1.32349	63
1	2	1.17024	1.14464	100
2	3	0.84111	0.82271	200
3	4	1.52348	1.02760	63
1	5	2.01317	1.35790	200
5	6	1.68671	1.13770	200
5	7	2.55727	1.72490	100
1	8	1.0882	0.73400	100
8	9	1.25143	0.84410	63
2	10	1.79553	1.21110	200
10	11	2.44845	1.65150	100
11	12	2.01317	1.35790	63
3	13	2.23081	1.50470	100
3	14	1.19702	0.80740	200
14	15	1.19702	0.80740	-----

TABLE II. POWER FLOW PARAMETERS

Nominal Voltage (kV)	Substation Power (kVA)	Toler.	Maximum Iterations	Power Factor	Maximum Energy Price (€/MWh)
11	2000	0.00001	20	0.9	120

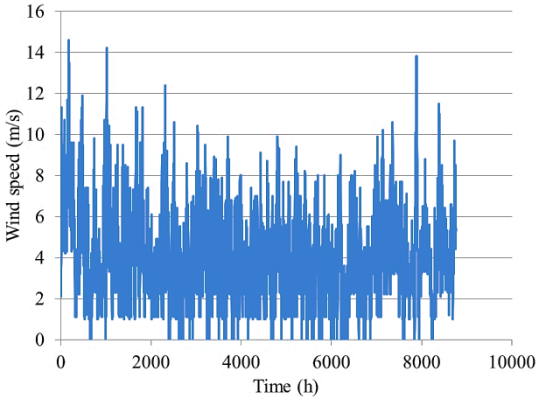

Figure 5. Wind speed time series.

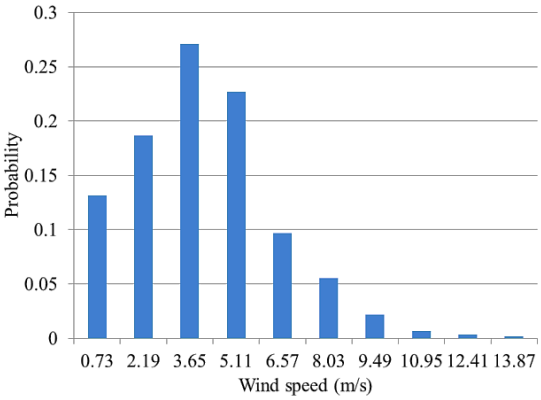

Figure 6. Probability distribution of wind speed.

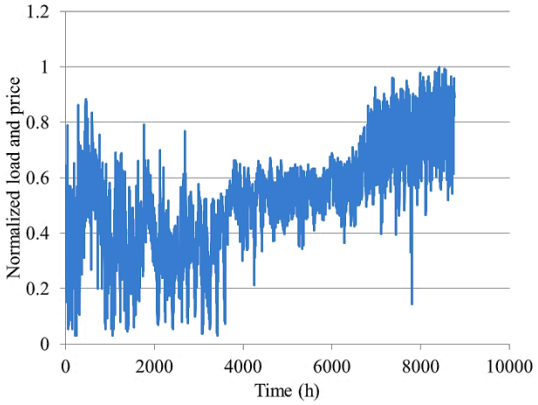

Figure 7. Reference time series *d*.

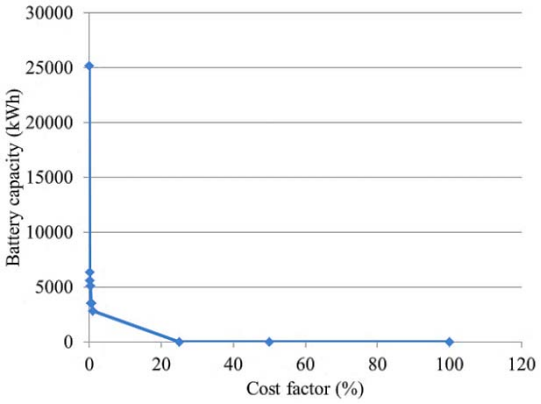

Figure 8. Sensitivity analysis over the VRFB cost.

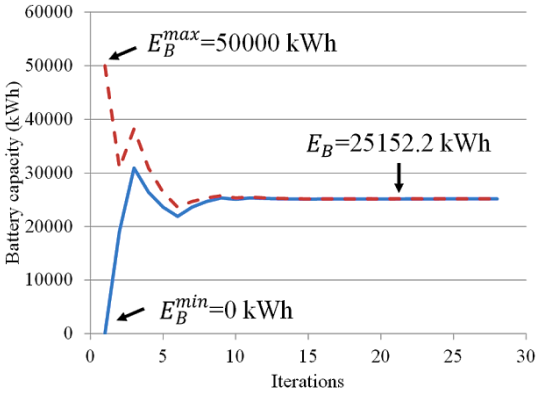

Figure 9. Behavior of GSSA.

Following the procedure detailed in Section IV, the rated capacity of the cell stack was set to 700 kW ($P_B^{max} = 700$ kW), the minimum and maximum settings of SOC on the charge controller were set to 0.15 ($SOC_B^{min} = 0.15$) and 0.9 ($SOC_B^{max} = 0.9$), respectively. The method converges to a BESS capacity of 25152.2385 kWh ($E_B = 25152.2$ kWh).

In Fig. 10 and 11, hourly values of VRFB SOC and power throughout the year show that VRFB charging and discharging occurs only between ($0\ h \leq t \leq 4000\ h$, approx.), i.e., when the load demand is relatively low (refer to Fig. 7). Fig. 12 shows the probability distribution of power supplied by the substation ($P_{SU(t)}\ \forall\ t = 1, \ldots, 8760$).

Two operating conditions are presented, with and without installing VRFB. When the VRFB is not installed, a significant amount of power has to be dissipated through the dump load in order to preserve the energy balance.

However, when VRFB is adopted, excess power generated consumed by the dump load is considerably reduced. In addition, the power supplied by the substation is reduced due to the availability of discharging process of BESS when needed.

Implementation was done using MATLAB® on a standard PC equipped with an i7-3630QM CPU at 2.40 GHz, 8 GB of RAM and 64-bit operating system. The computational time required to run the entire simulations was 8.35 minutes.

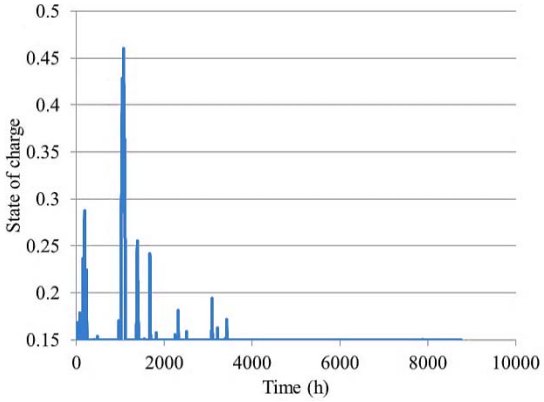

Figure 10. State of charge time series.

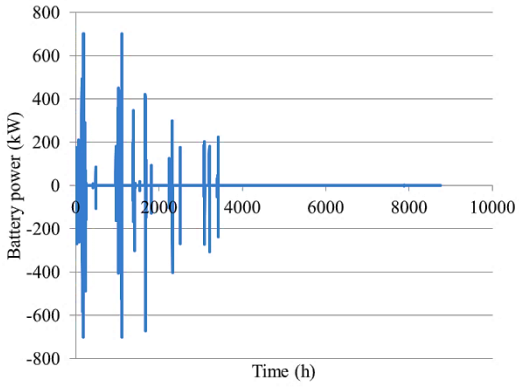

Figure 11. Battery power time series.

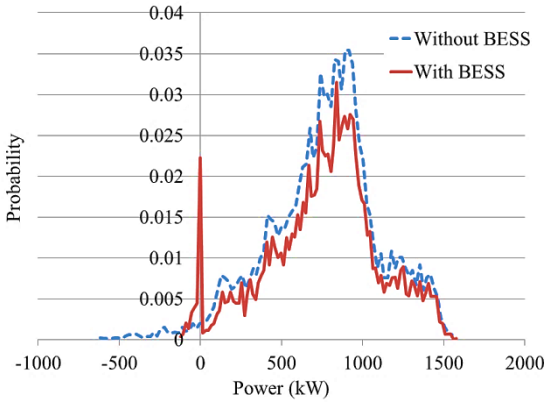

Figure 12. Probability distribution of substation power.

VI. Conclusion

In this work, an optimization model based on GSSA for optimal sizing of VRFB has been proposed in order to reduce the reverse power flow at a distribution system substation. The developed model considers yearly time series of renewable resources, load demand, and electricity prices within a probabilistic power flow framework. The effects of DG and reactive power compensation, as well as the influence of charge controller and power converter on VRFB operation have been taken into account. The optimization model was mathematically formulated to minimize NPC related to the installation of VRFB and the power to be supplied by the substation. According to the results obtained from the analysis of an illustrative example, it was concluded that the acquisition costs of VRFB are generally too high to be economically successful. However, the adoption of VRFB can improve the technical performance of the energy system, considerably.

Acknowledgment

J.P.S. Catalão acknowledges the support by FEDER funds through COMPETE 2020 and by Portuguese funds through FCT, under SAICT-PAC/0004/2015 (POCI-01-0145-FEDER-016434) and 02/SAICT/2017 (POCI-01-0145-FEDER-029803), whilst G.J. Osório acknowledges UID/EMS/00151/2019.

References

[1] A. G. Olabi, "Renewable energy and energy storage systems," *Energy*, vol. 136, pp. 1-6, Oct. 2017.

[2] Y. Cai, T. Huang, E. Bompard, Y. Cao, Y. Li, "Self-sustainable community of electricity prosumers in the emerging distribution system," *IEEE Trans. Smart Grid*, vol. 8, no. 5, pp. 2207-2216, Sept. 2017.

[3] A. Saint-Pierre and P. Mancarella, "Active distribution system management: A dual-horizon scheduling framework for DSO/TSO interface under uncertainty," *IEEE Trans. Smart Grid*, vol. 8, no. 5, pp. 2186-2197, Sept. 2017.

[4] Y. Zheng, J. Zhao, Y. Song, F. Luo, K. Meng, J. Qiu, D. J. Hill, "Optimal operation of battery energy storage system considering distribution system uncertainty," *IEEE Trans. Sust. Energy*, vol. 9, no. 3, pp. 1051-1060, Jul. 2018.

[5] E. Reihani, S. Sepasi, L. R. Roose, M. Matsuura, "Energy management at the distribution grid using a battery energy storage system," *Elect. Power Energy Syst.*, vol. 77, pp. 337-344, May 2016.

[6] E. Grover-Silva, R. Girard, G. Kariniotakis, "Optimal sizing and placement of distribution grid connected battery systems through an SOCP optimal power flow algorithm," *Applied Energy*, vol. 219, pp. 385-393, 2018.

[7] R. Seguin, J. Woyak, D. Costyk, J. Hambrick, B. Mather, "High-penetration PV integration handbook for distribution engineers," NREL *Technical Report NREL/TP-5D00-63114*, Jan. 2016.

[8] P. Giorsetto, K. F. Utsurogi, "Development of a new procedure for reliability modeling of wind turbine generators," *IEEE Trans. Power Appar. Syst.*, vol. PAS-102, no. 1, pp. 134-143, Jan. 1983.

[9] Y. Xu, F. Li, "Adaptive PI control of STATCOM for voltage regulation," *IEEE Trans. Power Deli.*, vol. 29, no. 3, pp. 1002-1011, Jun 2014.

[10] J. H. Teng, "Modelling distributed generations in three-phase distribution load flow," *IET Gen. Trans. Distr.*, vol. 2, no. 3, pp. 330-340, May 2008.

[11] G. J. Osório, E. M. G. Rodrigues, J. M. Lujano-Rojas, J. C. O. Matias, J. P. S. Catalão, "New control strategy for the weekly scheduling of insular power systems with a battery energy storage system," *App. Energy*, vol. 154, pp. 459-470, Sept. 2015.

[12] J. M. R. Fernández, M. B. Payán, J. M. R. Santos, Á. L. T. García, "The voluntary price for the small consumer: real-time pricing in Spain," *Energy Pol.*, vol. 102, pp. 41-51, Mar. 2017.

[13] Y. Fu, Q. Zhu, "Joint optimization methods for nonconvex resource allocation problems of decode-and forward relay-based OFDM networks," *IEEE Trans. Veh. Tech.*, vol. 65, no. 7, pp. 4993-5006, Jul. 2016.

[14] Y. Xu, C. Shen, Z. Ding, X. Sun, S. Yan, G. Zhu, Z. Zhong, "Joint beamforming and power-splitting control in downlink cooperative SWIPT NOMA systems," *IEEE Trans. Sign. Proc.*, vol. 65, no. 18, pp. 4874-4886, Sept. 2017.

[15] Y. Hongxing, Z. Wei, L. Chengzhi, "Optimal design and techno-economic analysis of a hybrid solar-wind power generation system," *Appl. Energy*, vol. 86, pp. 163-169, Feb. 2009.

[16] D. Das, D. P. Kothari, A. Kalam, "Simple and efficient method for load flow solution of radial distribution networks," *Inter. J. Elect. Power Energy Syst.*, vol. 17, no. 5, pp. 335-346, Oct. 1995.

[17] Royal Netherlands Meteorological Institute, KNMI Hydra Project. Accessed on 14/10/2018. [Online]. Available: http://www.knmi.nl/samenw/hydra

[18] Red Eléctrica de España, Markets and Prices. Accessed on 14/10/2018. [Online]. Available: http://www.ree.es/en

[19] M. Moore, R. Counce, J. Watson, T. Zawodzinski, "A comparison of the capital costs of a vanadium redox-flow battery and a regenerative hydrogen-vanadium fuel cell," *Adv. Chem. Engineering*, vol. 5, no. 4, pp. 1-3, Oct. 2015.